

Interplay of Chain Dynamics and Ion Transport on Mechanical Behavior and Conductivity in Ionogels

Mengze Lu^{1, 2#}, Wei Zhen Lian^{1, 2#}, Zhenhua Xiao^{1, 2}, Lu Liu^{1, 2}, Zhiwei Fan^{1, 2}, Xiaolin Jin^{1, 2},
Chuanxia Jiang³, Chen Qian⁴, Zheng-Hai Tang⁵, Panchao Yin^{1, 2}, Taolin Sun^{1, 2, 6, 7*}

¹South China Advanced Institute for Soft Matter Science and Technology, School of Emergent Soft Matter, South China University of Technology, Guangzhou 510640, China.

²Guangdong Provincial Key Laboratory of Functional and Intelligent Hybrid Materials and Devices, South China University of Technology, Guangzhou 510640, China.

³Guangdong Marubi Biotechnology Co., Ltd. No 92 Banhe Road, Huangpu District, Guangzhou, 510700, China

⁴School of Materials Science & Engineering, Zhejiang Sci-Tech University, Hangzhou 310018, P. R. China

⁵Department of Polymer Materials and Engineering, South China University of Technology, Guangzhou 510640, China

⁶Guangdong Basic Research Center of Excellence for Energy and Information Polymer Materials, South China University of Technology, Guangzhou 510640, China

⁷State Key Laboratory of Pulp and Paper Engineering, South China University of technology, Guangzhou, Guangzhou 510640, China

* Email: suntl@scut.edu.cn

Equal contributions

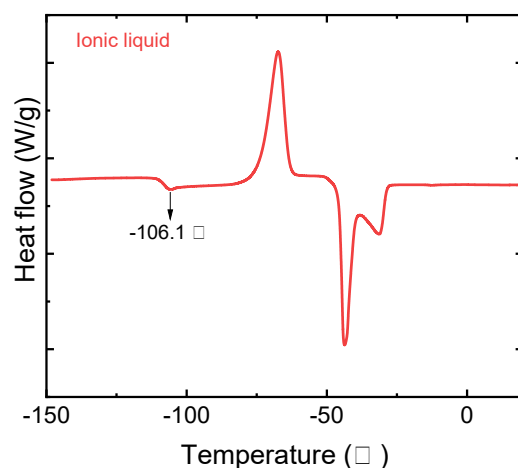


Figure S1 DSC traces of ionic liquid and P(DMAA-co-MAAc) matrix.

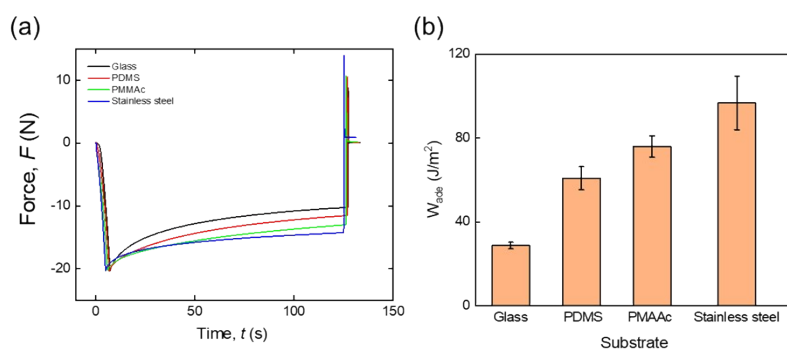


Figure S2 (a) Debonding force versus time curves on different substrates collected from probe-tack tests. (b) Adhesive energy W_{ade} of samples on different substrates, including glass, PDMS (Polydimethylsiloxane) and PMMA (Polymethyl methacrylate), and stainless steel.

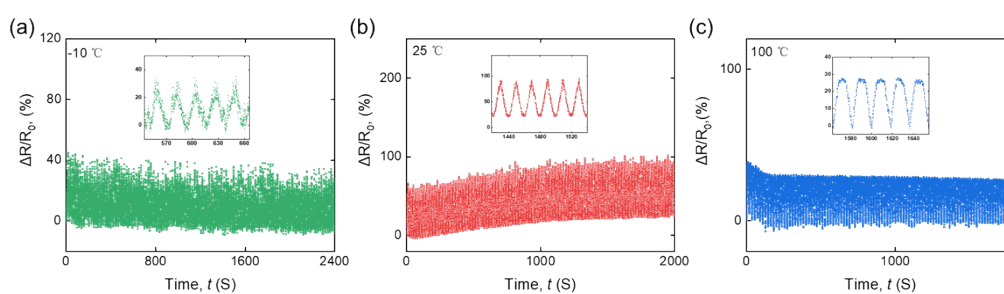


Figure S3 Resistance changes rate of the flexible strain sensor base on ionogel-0.8 at (a) $-10\text{ }^{\circ}\text{C}$, (b) $25\text{ }^{\circ}\text{C}$, and (c) $100\text{ }^{\circ}\text{C}$.

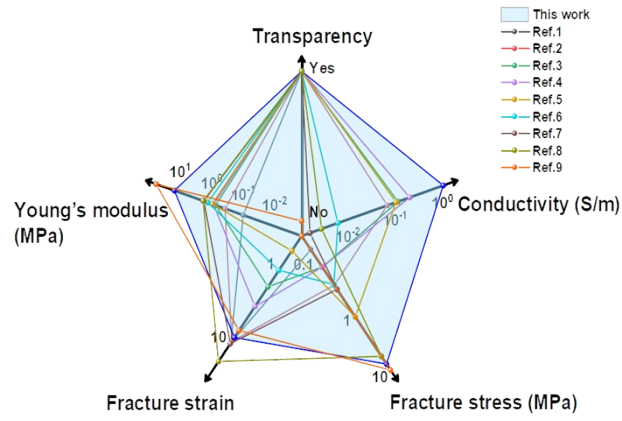


Figure S4 Rough comparison between this work and previously reported ionogel materials in terms of transparency, conductivity, stretchability, mechanical strength, and toughness¹⁻⁹.

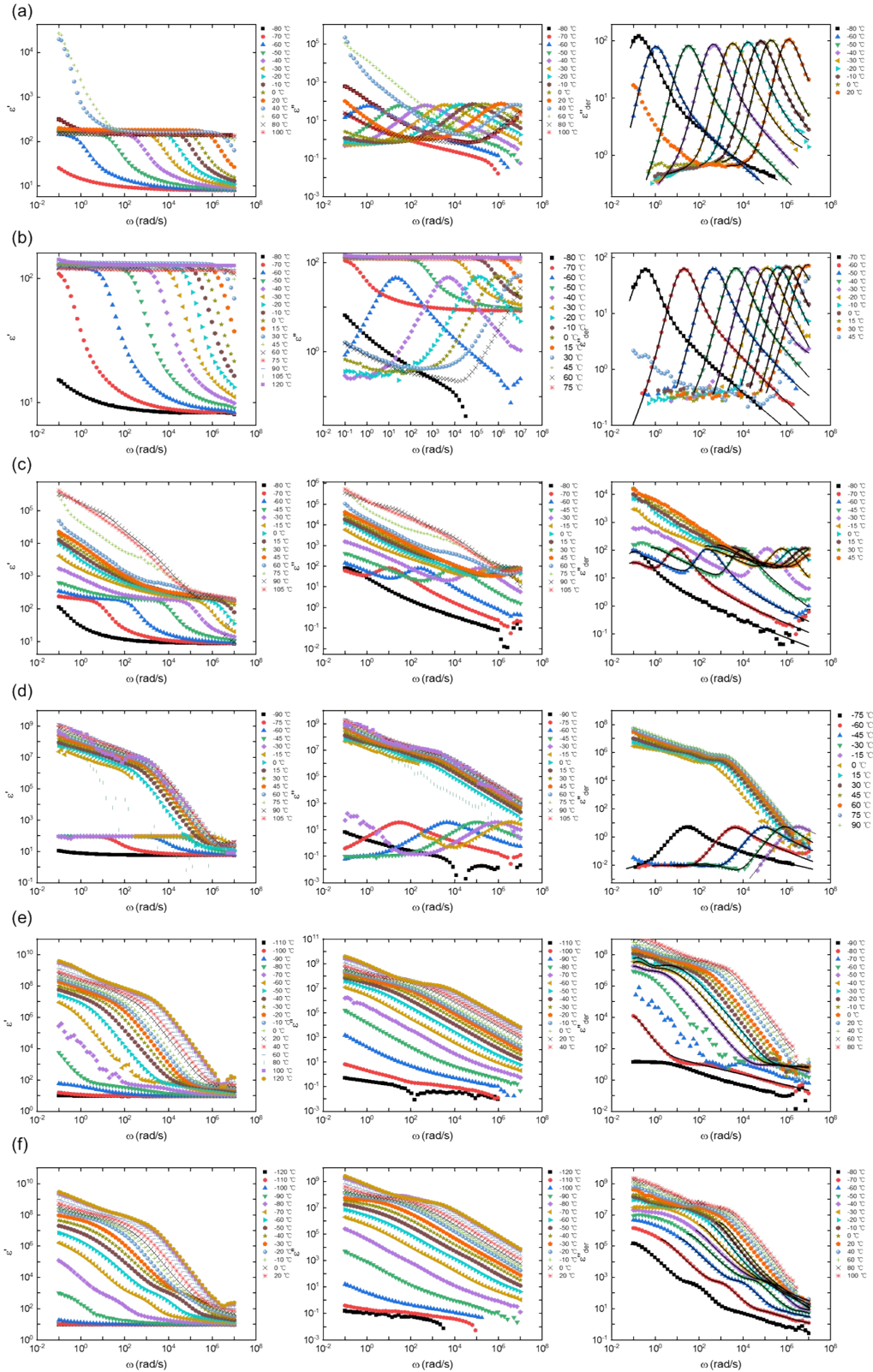


Figure S5 Isothermal plots of real part, ϵ' , imaginary part, ϵ'' and dc conduction free dielectric loss, ϵ''_{der} of the complex permittivity (ϵ^*) as a function of applied frequency, respectively, for (a) ionogel-0.65, (b) ionogel-0.7, (c) ionogel-0.75, (d) ionogel-0.8, (e) ionogel-0.85 and (f) ionogel-0.9. The solid lines through the ϵ''_{der} plots show the fitting of experimental data to HN formalism.

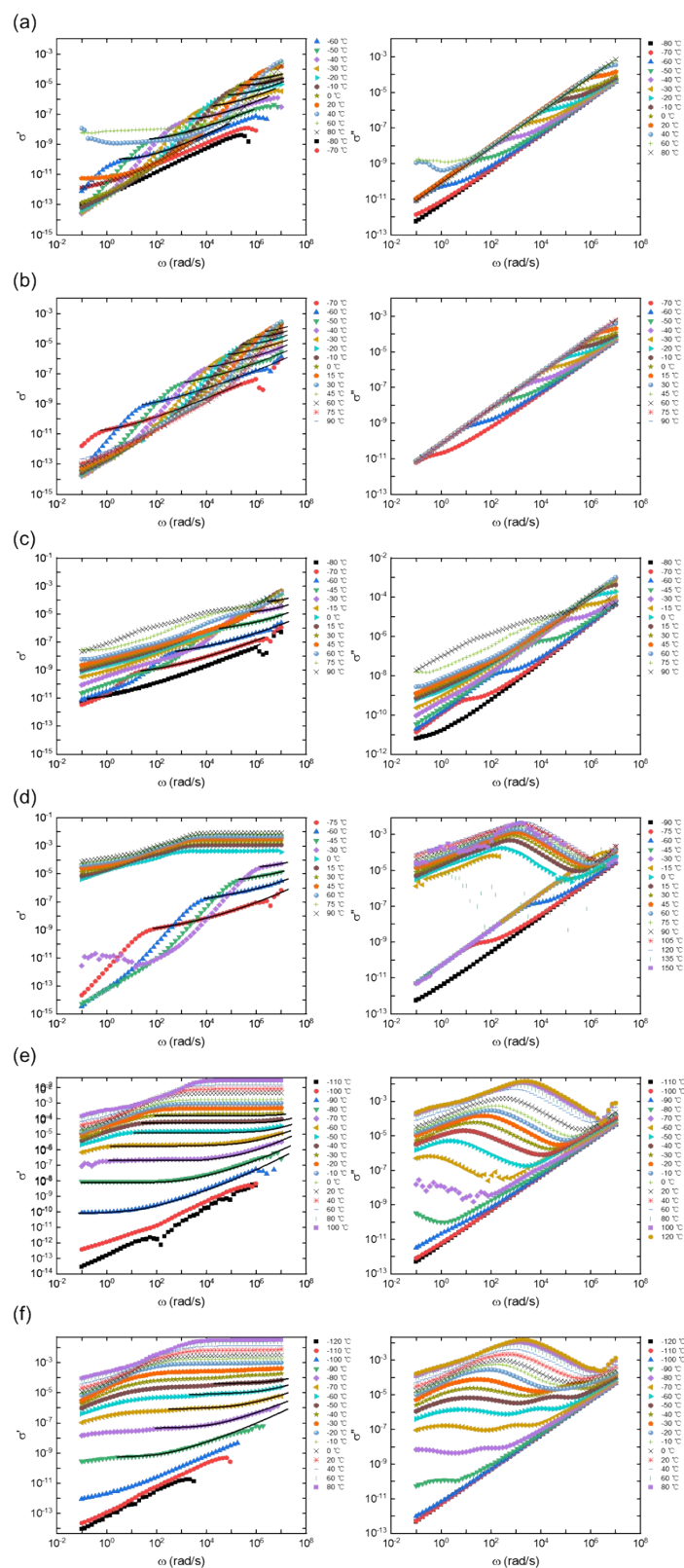


Figure S6 Isothermal plots of real part, σ' and imaginary part, σ'' of the complex conductivity (σ^*) as a function of applied frequency, respectively, for (a) ionogel-0.65, (b) ionogel-0.7, (c) ionogel-0.75, (d) ionogel-0.8, (e) ionogel-0.85 and (f) ionogel-0.9. The solid lines through the σ' plots show the fitting of experimental data to RBM formalism.

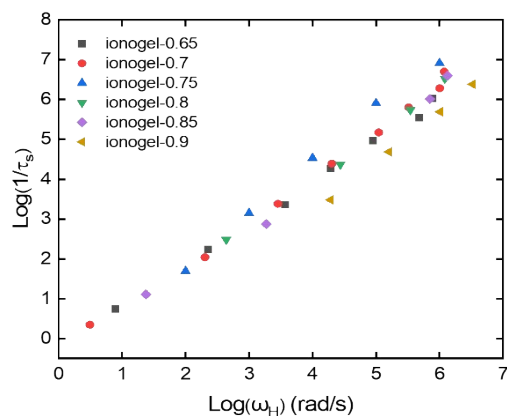


Figure S7 Plots of the inverse of segment relaxation time ($1/\tau_s$) versus hopping frequency (ω_H) of ionogel-m (m: 0.65-0.9).

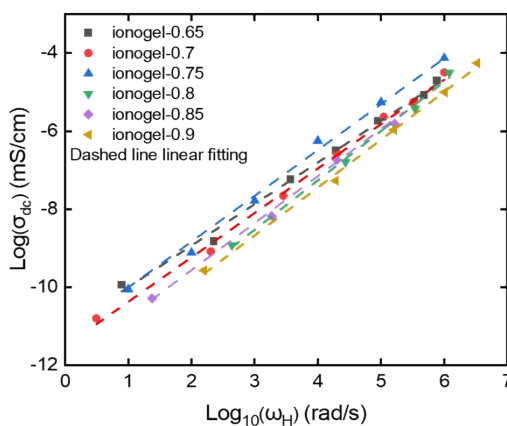


Figure S8 Plots of dc conduction σ_{dc} vs hopping frequency ω_H of these ionogels. The dashed lines represent the linear fitting of ionogel-m (m: 0.65-0.9).

Table S1 Slope of the plots of dc conduction σ_{dc} vs hopping frequency ω_H of ionogel-m (m: 0.65-0.9).

	Slope
ionogel-0.65	1.07
ionogel-0.7	1.14
ionogel-0.75	1.11
ionogel-0.8	1.26
ionogel-0.85	1.26
ionogel-0.9	1.23

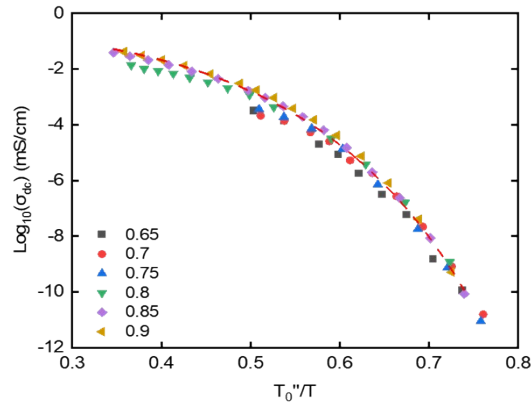


Figure S9 Normalized inverse of temperature dependent ionic conductivity (σ^{dc}) using the Vogel temperature T_0'' for all the ionogel-m (m: 0.65-0.9).

Table S2 WLF fitting constants C_1 and C_2 of temperature dependent the natural logarithmic plot of the horizontal shift factors a_T of ionogel-0.14-m (m: 0.65-0.9).

	C_1	C_2
ionogel-0.65	9.82	260.47
ionogel-0.7	10.56	160.83
ionogel-0.75	11.4	242.06
ionogel-0.8	10.93	231.17
ionogel-0.85	3.99	175.78
ionogel-0.9	1.33	131.44

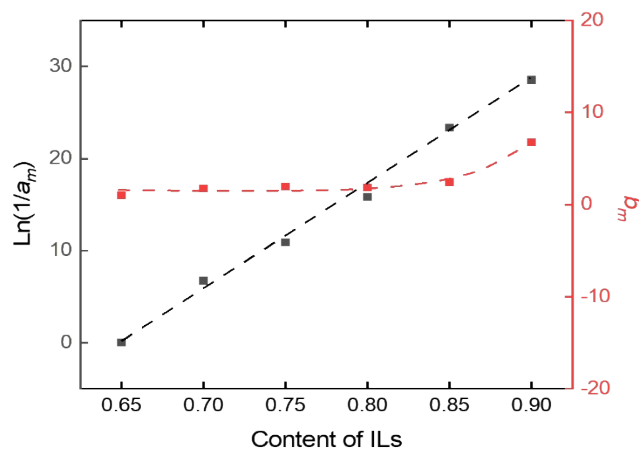


Figure S10 Time-concentration horizontal shift factor a_m (black plots) and vertical shift factor b_m (red plots) as a function of ionic liquid contents m. Reference content $m=0.65$.

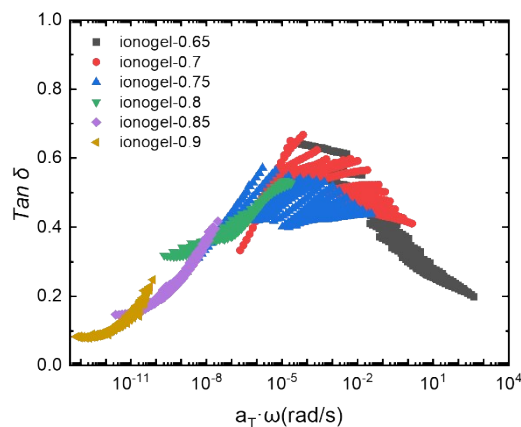


Figure S11 Loss factor $Tan \delta (= \frac{G''}{G'})$ following the principle of time-concentration superposition of all the ionogel-m (m: 0.65-0.9).

Table S3 Vertical shift-factor (a_s) of inverse of segmental relaxation time ($1/\tau_m$) of ionogel-0.14-m (m: 0.65-0.9) in Figure 7.

	a_s
ionogel-0.65	4.23
ionogel-0.7	6.96
ionogel-0.75	9.76
ionogel-0.8	11.96
ionogel-0.85	11.41
ionogel-0.9	8.65

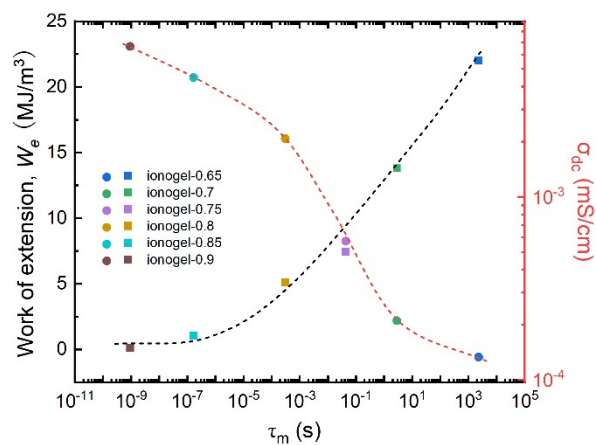


Figure S12 The relationship between the work of extension and conductivity and segment

relaxation time.

References:

1. Yiming B, Han Y, Han Z, et al. A mechanically robust and versatile liquid-free ionic conductive elastomer[J]. *Advanced Materials*, 2021: 2006111.
2. Li R A, Chen G, He M, et al. Patternable transparent and conductive elastomers towards flexible tactile/strain sensors[J]. *Journal of Materials Chemistry C*, 2017, 5 (33): 8475-8481.
3. Ou Y, Zhao T, Zhang Y, et al. Stretchable solvent-free ionic conductor with self-wrinkling microstructures for ultrasensitive strain sensor[J]. *Materials Horizons*, 2022.
4. Kim Y M, Moon H C. Ionoskins: Nonvolatile, highly transparent, ultrastretchable ionic sensory platforms for wearable electronics[J]. *Advanced Functional Materials*, 2020, 30 (4): 1907290.
5. Yiming B, Guo X, Ali N, et al. Ambiently and mechanically stable ionogels for soft ionotropic[J]. *Advanced Functional Materials*, 2021, n/a (n/a): 2102773.
6. Li M, Li J, Na H, et al. Mechanical behavior of poly (methyl methacrylate)-based ionogels[J]. *Soft Matter*, 2014, 10 (40): 7993-8000.
7. Zhang Y, Li M, Qin B, et al. Highly transparent, underwater self-healing, and ionic conductive elastomer based on multivalent ion–dipole interactions[J]. *Chemistry of Materials*, 2020, 32 (15): 6310-6317.
8. Liu J, Chen Z, Chen Y, et al. Ionic conductive organohydrogels with dynamic pattern behavior and multi-environmental stability[J]. *Advanced Functional Materials*, 2021, 31 (24): 2101464.
9. Wang M, Zhang P, Shamsi M, et al. Tough and stretchable ionogels by in situ phase separation[J]. *Nature Materials*, 2022.